

Performance of Embedded Fiber Optic Sensors in Composite Structures

Falah M. Wegian¹⁾, Falah A. Almottiri²⁾

¹⁾ Assistant Prof., Civil Engineering Department, College of Technological Studies, P.O. Box: 27590 Safat, 13136 Kuwait, fmwm@yahoo.com

²⁾ Assistant Prof., Civil Engineering Department, College of Technological Studies, falah13@hotmail.com

ABSTRACT

The technology of fiber optic sensors, initially developed for use in aerospace industry, is currently investigated for its applicability in civil engineering. Advances in the structural application of this technology will facilitate the use of built-in monitoring capability in reinforced concrete members, and consequently enable the production of smart structures. This paper investigates the development of a Fiber Optic Bragg Grating Sensor (FOBGS) for embedding in concrete members to measure strain and monitor cracks. Tests were carried out on a steel plate subjected to flexural stress and reinforced concrete beams subjected to axial tensile stress and temperature change. The FOBGS was employed to track the behaviour of these members under loading conditions. A theoretical analysis was performed on the tested specimens to estimate strain values and cracking loads. Good agreement was found between the theoretical and the experimental results.

KEYWORDS: Concrete, Cracking, Fiber Optic Sensors, Strain.

1. INTRODUCTION

Highway bridge decks and parking structures are prime examples of structures subjected to severe environmental and loading conditions, leading to the deterioration of the main structural concrete components. In Canada, it is estimated that the cost of repair of parking structures is in the range of four to six billion dollars¹ (Bédard, 1992). The estimated repair cost for existing highway bridges in the United States is over 50 billion dollars, and one to three trillion dollars for all concrete structures² (Fickelhorn 1990). Excessive corrosion problems also exist in Arabian Gulf countries^{3,4} (Makhtouf et al.,1991; Doncaster et al.,1996) The exterior of reinforced concrete structures in these countries is subjected to an extremely aggressive environment due to high temperatures and humidity.

Engineers are currently exploring the use of Fiber Optic Sensors (FOSs) to develop a remote network that can monitor many bridge sites from a central location. This will allow for real-time and long-term identification of the structural behaviour from records obtained by FOSs fixed at critical locations of a structure, hence saving time and money spent on physical on-site inspection. The monitoring system can also be configured through an alarm feature to provide warning to allow repair before damage becomes excessive.

FOSs are resistant to corrosion and immune to electromagnetic interface. These properties make them more suitable than the conventional foil strain gauges for remote sensing within large structures that are subject to lightning or man-made sources of electric interference. The small size of FOSs, linear geometry and dielectric nature also make them readily embeddable in advanced composite materials currently used for reinforcing concrete members. Although the conventional strain

Received on 3/10/2006 and Accepted for Publication on 18/12/2006.

gauges are sensors with a long history that attests to their reliability, their use is limited to external applications and short-term readings since their working life-time is only about two years⁵ (Gu et al., 2000).

2. THE FOBGS SYSTEM

An example of a particularly useful application of an FOBGS is the distributed strain sensor⁶ (Measures, 1996), in which an optical fiber having a series of gratings with different Bragg periods is embedded, or adhesively attached to a structure undergoing stress. Each grating serves as an independent strain sensor. Minute displacements in portions of the structure cause corresponding changes in the Bragg period in the gratings coupled to those portions of the structure. These changes in the Bragg period can be detected as changes in the spectrum of the light reflected by the gratings.

This FOBGS system measures the axial strain distribution along a grating that can range from 3 mm to 100 mm length⁷ (Huang et al., 1996). The length of the grating can be thought of as the gauge length over which the average strain is determined. In the work discussed in this paper, the gauge length was 10 mm, however this length can be varied depending on the specific application. A fiber optic Bragg grating is a periodic variation in the index of refraction along a certain length of the core of a single mode optical fiber. When broadband light is launched into this fiber, a narrow band of light will be reflected back by the grating. The central reflected wavelength λ is given by⁸ (Wegian, 2001):

$$\lambda = 2n\Lambda; \quad (1)$$

where Λ is the length of the grating period, and n is the average index of refraction of the fiber core. If the grating is subject to a strain, both Λ and n will change leading to an increase or a decrease in the reflected wavelength λ . In case of uniform strain along the grating, all periods will reflect the same λ that can be used to determine the applied strain. However, if the strain field varies along the grating (e.g. in x-direction), the reflected wavelengths will become⁸ (Wegian, 2001):

$$\lambda(x) = 2n(x)\Lambda(x) = 2n_o\Lambda_o[1 + a\varepsilon(x)]; \quad (2)$$

where:

$$a = 1 - 0.5n_o^2[p_{12} - \nu(p_{11} + p_{12})]; \quad (3)$$

where n_o and Λ_o are the original values of the average index of refraction and the period of the grating, respectively when $\varepsilon(x)$ equals to zero; p_{11} and p_{12} are the strain-optic constants for the optical fiber, and ν is the Poisson's ratio.

Each fiber optic sensor has a pre-measured gauge factor and a calibrated wavelength specification, which are provided by the supplier. These values have to be programmed in the fiber optic strain indicator to obtain accurate results. In this research, the FOBGS system shown in Figure 1 was set up to transverse data from each BG sensor at every change in strain during loading. The ability of a BG sensor to measure strain and crack width depends on the change in the BG wavelength resolution of the demodulator. As shown in Figure 1, the fiber optic sensor consists of three layers, namely; a core of 9 microns, a cladding of 125 microns and a coating of 250 microns. The length of the BG sensors used in the experimental program was 10 mm. The BGS had a bandwidth of (-3 dB), where dB is the abbreviation for decibel, which is a logarithmic expression of the ratio between two signal power levels. The original wavelength was $\lambda_o = 1308740$ pm at a gauge factor $GF = 0.77$ and a maximum lead sensitivity of $\pm 5 \mu\varepsilon$.

3. EXPERIMENTAL PROGRAM

In this research, tests were conducted on five specimens. These include one steel plate subjected to flexural stresses, two reinforced concrete beams subjected to temperature change and two reinforced concrete beams subjected to axial tensile stress. The strains measured using the FOBGS were compared to the theoretical strains. The cracks in the concrete specimens were monitored using the installed FOBGS.

3.1 Steel Plate Test:

A steel plate of 736.6 x 25.4 x 6.35 mm was tested as a cantilever fixed at one end and free at the other end.

The plate was subjected to a vertical concentrated load at the free end with a cantilever span of 376 mm. An

FOBGS was installed at the distance of 63.5 mm from the fixed end. The tensile strain was monitored with an

Table 1- Theoretical Strains and BG Measured Strains for the Steel Plate Test.

Load (N)	Theoretical		BG	BG
	Strain ($\mu\epsilon$)	Voltage (V)	Wave length (pm)	Strain ($\mu\epsilon$)
5	49	3.90	1308821	50
10	98	3.75	1308927	100
15	147	3.63	1309012	155
20	196	3.50	1309100	210
25	245	3.37	1309188	260
30	294	3.23	1309285	310
35	343	3.09	1309390	363
40	392	2.98	1309470	415
45	441	2.86	1309556	472
50	490	2.73	1309649	533

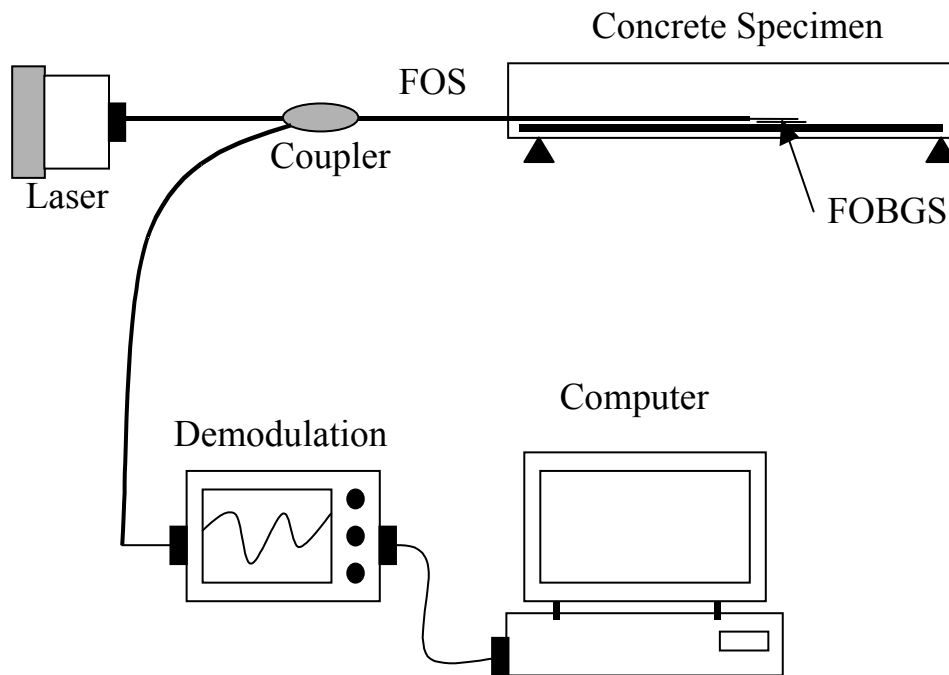


Fig. 1. Fiber Optic Bragg Grating Sensor System.

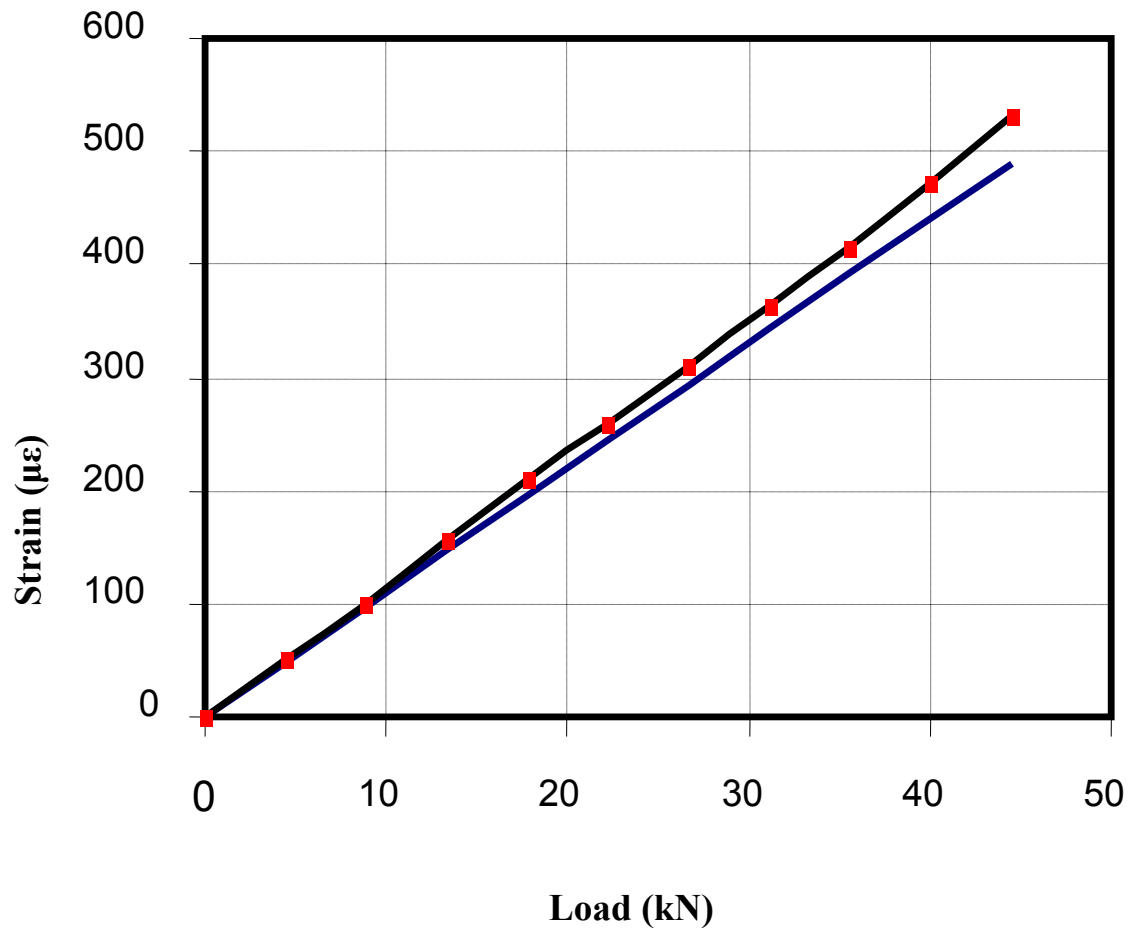


Fig. 2. Tensile Strain in the Tested Steel Plate.

incremental load increase from 5 N to 50 N. The temperature during this test was kept constant at 25° C. The objective of this test was to examine the performance and the results of the FOBGS before using it in the reinforced concrete specimens.

Figure 2 shows the measured strains using the fiber optic sensor. The theoretical strains are plotted in the same figure for comparison purposes. Table 1 shows the voltage and wavelength readings during the experiment. The corresponding FOBGS measured strains and theoretical strains are also shown in Table 1. Figure 2 shows that the experimental tensile strain is almost linear. Comparing the experimental and the theoretical results, it can be seen that the measured strains were within a percentage of 5% higher than the theoretical strains. The maximum difference was noticed at the final load

increment.

3.2 Reinforced Concrete Beam Tests:

The layout of the reinforced concrete specimens is shown in Figure 3. The beams with a 160 mm x 160 mm cross-section and 1200 mm length were instrumented by embedded FOBGS to measure strain and monitor concrete cracks. Two specimens, T1 and T2, were subjected to temperature change test, and the remaining two specimens, L1 and L2, were subjected to axial tensile load up to failure. In specimens T1 and L1, the BG sensor was installed at mid-length of one of the main steel bars inside the concrete. In specimens T2 and L2, the BG sensor was attached to a steel plate embedded at the center of the concrete beam. The steel plate was welded to the adjacent stirrups before casting the concrete.

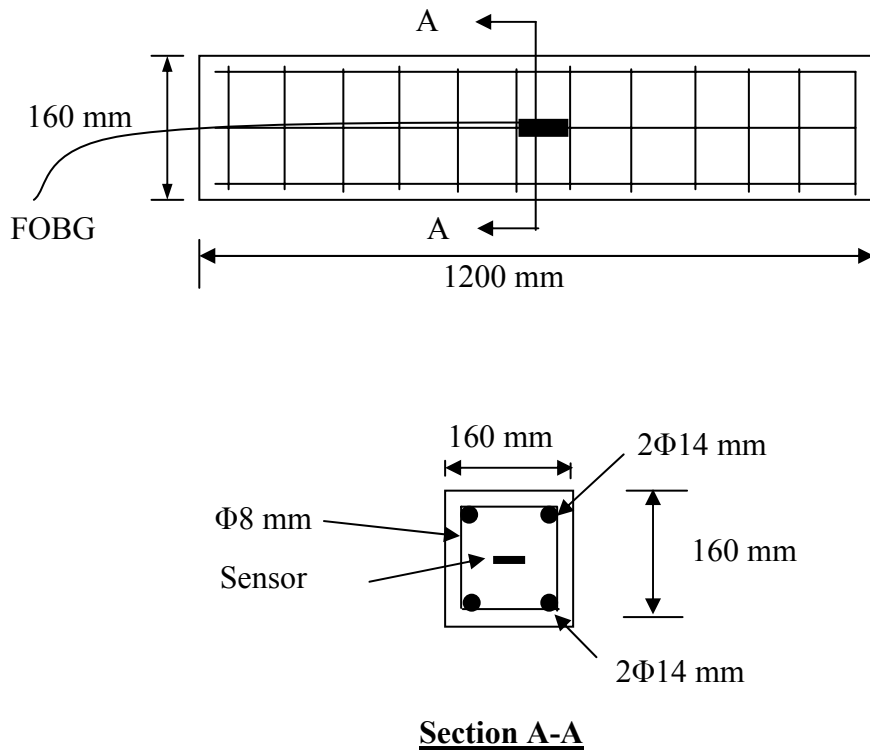


Fig. 3. Details of the Tested Reinforced Concrete Beams.

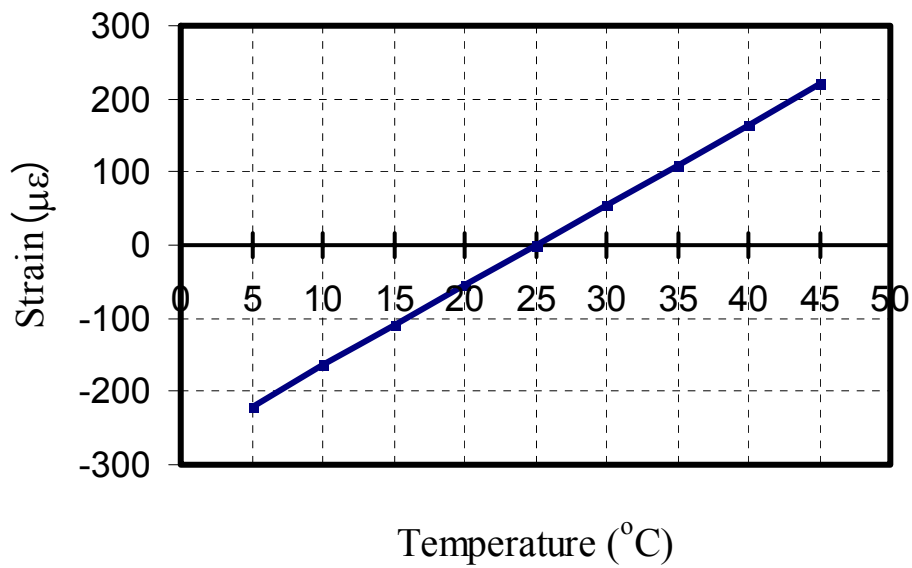


Fig. 4. FOBGS Strain Due to Temperature Change.

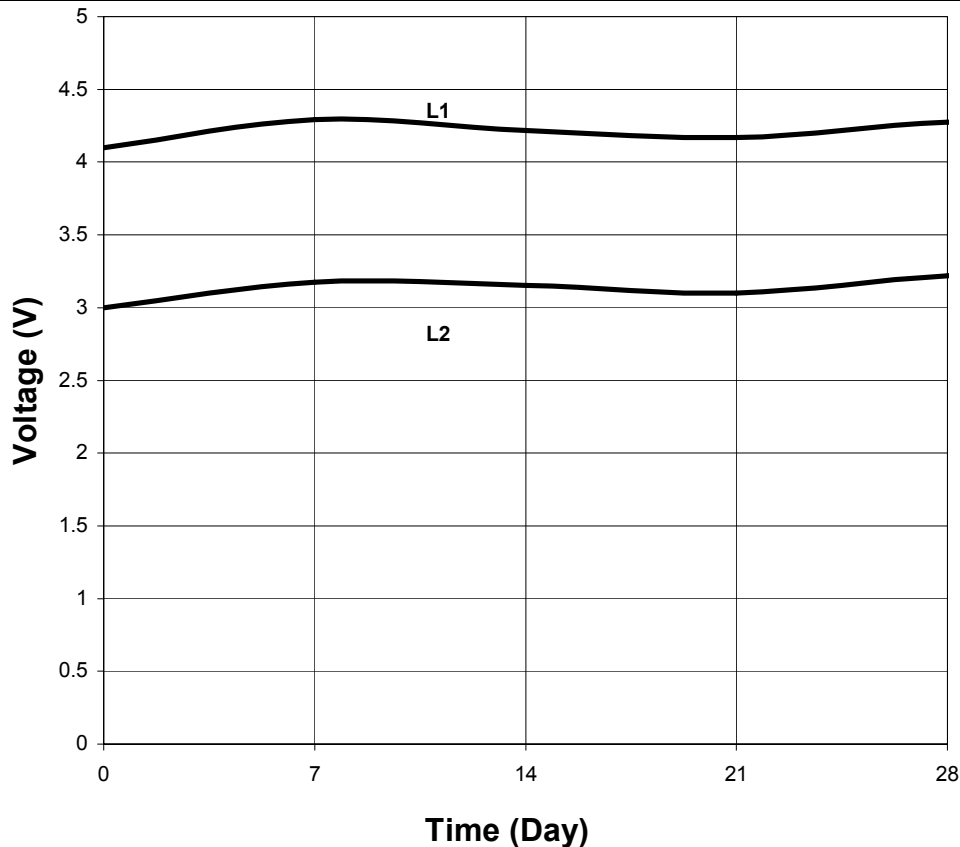


Fig. 5. BG Sensor Readings during the Curing Process.

The concrete was designed for a 7-day compressive strength of 30 MPa. The percentage of fine aggregate to total aggregate was 48%. The water-cement ratio was 0.4 with an aggregate-cement ratio of 2.7, both by weight. The maximum size of coarse aggregate was 10 mm. Stirrups of mild steel of 300 MPa nominal yield strength, were provided.

3.2.1 Temperature Change Test:

The objective of this test was to examine the temperature sensitivity of the FOBGS measurements. The reinforced concrete specimens T1 and T2 were tested in the climate chamber under a cycled temperature change. During the test, the temperature was increased from the room temperature of 25° C to 45° C in 4 hours, then decreased to 5 ° C in 8 hours, and finally increased again up to 25° C in 4 hours. The change in temperature was applied in increments of 5° C per hour. Figure 4 shows the FOBGS recorded strain results for

this test. It can be seen from Figure 4, that the relationship between strain and temperature increase is linear. The strain readings were not affected by the low or high temperatures within the experiment range. Therefore, BG sensors can be used for monitoring purposes in the field applications without any measurement interruptions in the normal weather conditions.

3.2.2 Axial Tension Test:

Before applying the tensile load test on specimens L1 and L2, their curing behaviour was examined. The concrete beams were fully submerged in water for 28 days. During this period, the FOBGS readings were recorded. The objective of this test was to examine the transmission of the FOBGS signal for long time and in the under-water conditions, and to monitor the behaviour of the specimens during the curing period. Figure 5 shows

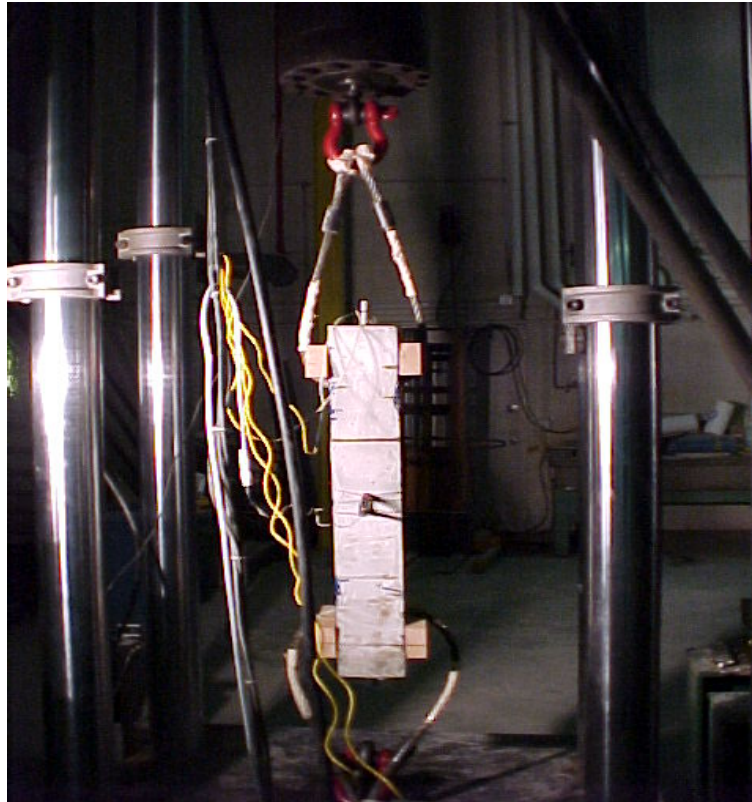


Fig. 6. Loading System for the Tested Concrete Beams.

the FOBGS readings for both specimens for the curing duration of 28 days. It can be seen that the voltage readings were increasing in the first 7 days of the test. It has to be mentioned that the increase in voltage denotes a decrease in strain. The readings were then fluctuating up and down starting from day 7 until day 28. Finally, the readings remained constant for the rest of the experiment. The results show that the variations in the FOBGS output took place in the first 28 days of the curing time. This is the curing period recommended by the codes of practice in concrete structures. Only minor changes occur in concrete strength after this period.

Specimens L1 and L2 were then prepared for the axial tensile test. The loading system consisted of a hydraulic power supply, a load cell, two carbon fiber reinforced polymer CFRP wires and two shackles as shown in Figure 6. A 500 kN closed-loop MTS actuator was used to apply the load through the upper and lower shackles.

Each CFRP wire was connected to a shackle at one end and to the specimen through a circular hole at the other end. The tensile loads were applied gradually from zero to 90 kN and then back to zero. The FOBGS strain history was recorded and plotted in Figure 7. The results show small strain values before concrete cracking. After cracking, the total load is practically carried by the reinforcing steel bars. Figure 7 shows that the total strain in the steel bars after concrete cracking was $900 \mu\epsilon$. Using the elastic theory, this value was estimated to be $862 \mu\epsilon$, assuming the elasticity modulus of the steel bars to be 200000 MPa. This indicates that the difference between the theoretical and the experimental strain was in the range of 4%.

3.2.3 Crack Monitoring Test:

During the axial tension test described above, the concrete cracking was monitored using the FOBGS. Figure 8

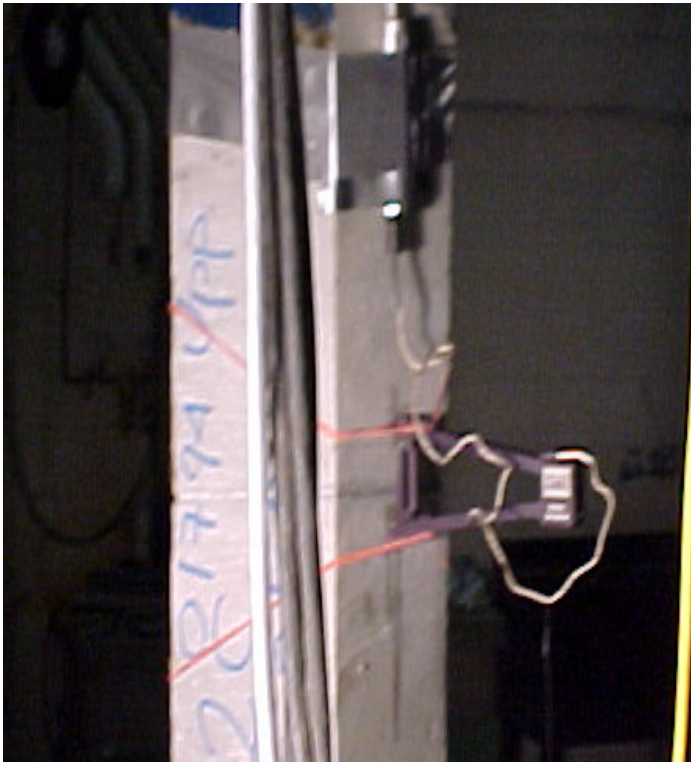


Fig. 7. Force –Strain History during the Axial Tension Test.

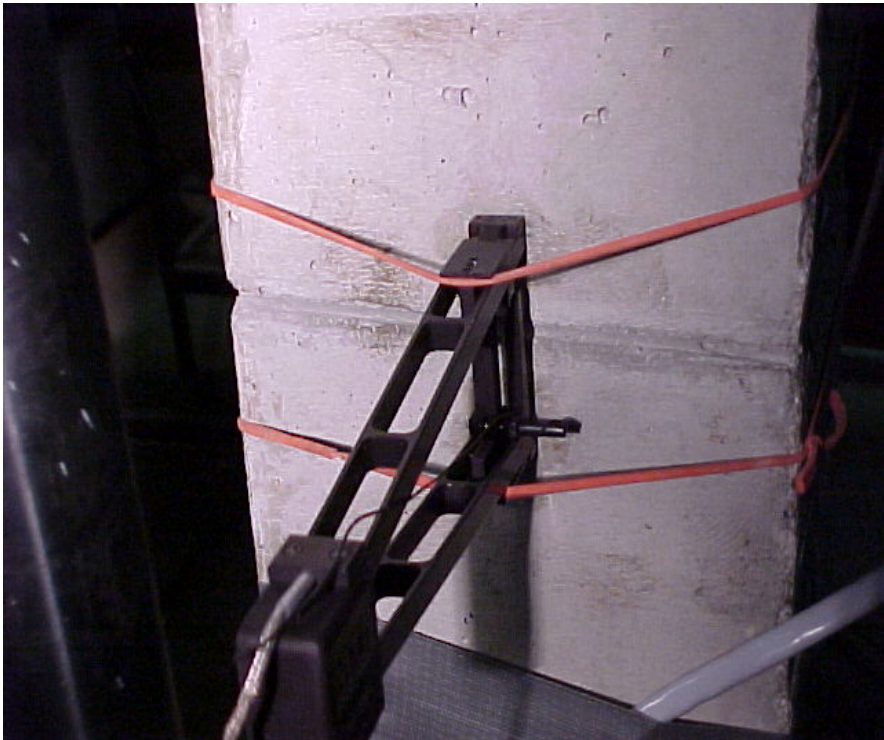


Fig. 8. Crack Propagation Pattern during the Tension Test.

shows the crack propagation pattern during the load increase. The following observations were recorded during the test:

- Crack openings less than 0.15 mm were not clearly detected by the BG crack sensor system. This was due to the negligible variation in the signal loss at this level of crack openings.
- Crack openings between 0.15 mm and 1.15 mm were clearly noticed by the BG crack sensor system. Figure 8 shows the history of the crack opening at the specimen mid-length. The variation in the signal loss clearly demonstrated the crack at a load of 52 kN.
- At a crack opening width greater than 1.15 mm, the signal loss started to drop down. This took place when the applied load reached the maximum value of 90 kN as shown in Figure 8.

It has to be mentioned that the above observations are true, provided that the longitudinal reinforcement did not yield, and the concrete did not completely fail during the experiment.

4. SUMMARY AND CONCLUSIONS

Measured strains of five steel and concrete specimens

REFERENCES

- Bédard, C. (1992). "Composite Reinforcing Bars: Assessing Their Use in Construction." *ACI Concrete International*, 14, (1), 1992, 55-59.
- Fickelhorn, M., (1990). "Materials and Structures." *RILEM*, 23 (137), Sept. 317.
- Makhtouf, H.M., Ahmadi, B.H. and Al-Jabal, J., (1991). "Preventing Reinforced Concrete Deterioration in the Arabian Gulf." *Concrete International*, 13 (5), May 1991, 65-67.
- Doncaster, A.M., Newhook, J.P and Mufti, A.A. (1996) "An Evaluation of Fiber Optic Sensors." *Proceedings of the 2nd. International Conference on Advanced Composite Materials in Bridges and Structures*, Montreal, Canada, Aug., 1011- 1021.
- Gu, X., Chen, Z. and Ansari, F., (2000) "Embedded Fiber Optic Crack Sensor for Reinforced Concrete Structures." *ACI Structural Journal*, 97 (3), May-June, 468-476.
- Measures, R.M., (1996). "Fiber Optic Sensor Instrumented Bridges – 21st Century Information Highways." *Proceedings of the 2nd. International Conference on Advanced Composite Materials in Bridges and Structures*, Montreal, Canada, Aug., 31- 40.
- Huang, S., LeBlanc, M., (1996). "Lowery, M., Maaskant, R. and Measures, R.M., Distributed Fiber Optic Strain Sensing for Anchorages and Other Applications." *Proceedings of the 2nd. International Conference on Advanced Composite Materials in Bridges and Structures*, Montreal, Canada, August, 991- 998.
- Wegian, F., (2001) *Concrete Structures – Analysis and Design*, Dar Arab, Kuwait, 1st edn., ch. 3, 22-33.
- Wegian, F., (2004) *Concrete Structures – Analysis and Design*, Dar Arab, Kuwait, 2nd edn., ch. 2, 9-1